The effects of elastic supports on the transient vibroacoustic response of a window caused by sonic booms

Dayi Ou and Cheuk Ming Mak[a)]
Department of Building Service Engineering, The Hong Kong Polytechnic University, Hung Hom, Kowloon, Hong Kong, China

(Received 27 December 2010; revised 13 May 2011; accepted 20 June 2011)

The transient vibration and sound radiation (TVSR) of plate-like structures with general elastic boundary conditions was investigated using the time-domain finite element method (TDFEM) and time-domain boundary element method (TDBEM). In this model, the structure can have arbitrary elastic boundary conditions and hence the effects of the boundary conditions on the TVSR can be effectively studied. The predicted results agreed well with existing experimental data using two classical boundary conditions: simply supported at all edges and clamped-free-free-free. The TVSR of a single panel with a more general boundary condition in two connected chambers was also measured. The predicted results agreed well with these experimental results. The prediction method was subsequently applied to evaluate the effects of elastic boundary supports on the TVSR of a window caused by a sonic boom. Loudness, non-audible acoustic perception, and tactile vibration thresholds were analyzed for different boundary conditions (varying between clamped and simply supported). The possibility of improving the transient vibration and noise isolation performance by selecting an appropriate boundary condition was thereby demonstrated.
 [DOI: 10.1121/1.3613696]

PACS number(s): 43.50.Pn, 43.28.Mw, 43.40.Dx, 43.55.Rg [DF] Pages: 783–790

I. INTRODUCTION

The effects of different boundary conditions on the vibration and sound radiation of plate-like structures have been studied for decades. Leissa reviewed the vibration properties of a thin plate with various classical boundary conditions, such as free, simply supported, and clamped.[1] With the development of various approximate and numerical solution techniques, studies on the effects of more general boundary conditions, such as arbitrary boundary supports with rotational and translational stiffness, have also been carried out.[2–4] These studies indicate that the properties of the boundary supports significantly affect the vibration and sound radiation of the plate.

But simplification of the vibration and sound radiation problem to a steady-state one by assuming harmonic excitations is usually different from the actual noise sources. Apart from studies of the steady state problems, other research has analyzed the transient response of plate-like structures.[5–12] In these studies, Forsyth and Warburton[11] analyzed the transient response of cantilever plates to an impulse force. Craggs[12] investigated the transient responses of clamped, simply supported, and cantilever plates using the transition matrix method. These studies suggest that boundary conditions significantly affect the transient response of a plate. Nevertheless, most studies have used classical boundary conditions. Few references can be found that deal with the transient response of a plate with general boundary conditions. Fan[13] is one investigator who has considered the effects of viscoelastic boundary supports on the transient vibration and sound radiation (TVSR) of a rectangular plate. But in his model, different beam mode shape functions are required to calculate the modal loss factor and the final modal equations for different boundary conditions; consequently, a specific set of characteristic functions for each type of boundary condition is required. Moreover, his model is not well suited for plates with arbitrary, non-uniform edge restraints. Since boundary conditions are important in the TVSR of plate-like structures, and since they have potential applications in optimizing structure mounting designs, a more systematic study of the effects of arbitrary boundary conditions on the TVSR of these structures is required.

Among the various types of transient excitations, a sonic boom is one type of shock wave that could transfer high levels of vibration and noise into residential buildings. The transient response of a plate-like structure caused by an N-wave has been widely studied.[12,14–17] One study carried out by Craggs[12] compared the vibration responses of a rectangular plate with all edges simply supported and one with all edges clamped; a notable difference could be seen between the two responses. This difference indicates that the effects of boundary supports cannot be ignored when dealing with this type of problem. But to our best knowledge, no results have been reported for the transient vibroacoustic responses of a window with arbitrary elastic boundary conditions caused by sonic booms.

The specific problem that motivated this study is that an effective tool is lacking for predicting the transient vibroacoustic response of a plate-like structure caused by sonic booms with arbitrary elastic boundary conditions. This study develops a numerical method based on the time-domain finite element method (TDFEM) and time-domain boundary element method (TDBEM). The elastic parameters along the

[a)]Author to whom correspondence should be addressed. Electronic mail: becmmak@polyu.edu.hk

plate contour could be arbitrarily varied to simulate different types of boundary conditions.

II. THEORETICAL FRAMEWORK

A. Theoretical model

Consider a thin rectangular plate of length L_x, width L_y and thickness h with arbitrary elastic boundary supports along the four edges, as shown in Fig. 1. The plate is mounted on an infinite rigid baffle, as shown in Fig. 2. Cartesian coordinates X, Y, and Z originate at the center of the plate, with X and Y parallel to its sides. The plate baffle system is immersed in an infinite light fluid medium (air) and separates the medium into receiver section $V_1(z > 0)$ and source section $V_2(z < 0)$. The plate is subject to a time varying input force $F(x, y, t)$. The classical thin plate theory is used to analyze the vibration of a plate, but does not take into account the effects of rotary inertia and shear deformation. The effect of fluid loading on the plate's vibration has also been neglected.

B. Vibratory motion of the plate

1. Time-domain finite element method (TDFEM)

The time-domain finite element method is used to determine the vibration response of this plate. The dynamic equilibrium equation[18] can be written as

$$\{M\}\{\ddot{u}\} + \{D\}\{\dot{u}\} + \{K\}\{u\} = \{F(t)\}, \tag{1}$$

where $\{M\}$, $\{D\}$, and $\{K\}$ are the mass, damping, and stiffness matrices, $\{F(t)\}$ is the time-dependent external load vector, and $\{u\}$, $\{\dot{u}\}$, and $\{\ddot{u}\}$ are the nodal displacement, velocity, and acceleration vectors. A proportional damping[19] $\{D\}$ is used here, where $\{D\}$ is assumed to be proportional to $\{K\}$ and is written as $\{D\} = \beta\{K\}$. $\beta = 2\eta/\omega_0$, η is the damping factor and ω_0 is the fundamental natural frequency of the plate system.

The four-node rectangle Kirchoff plate element[18] is used in the TDFEM model, and the mesh size of the element is determined by considering both the solution accuracy and computational cost. A suggestion proposed by Kim *et al.*[20] is a mesh size equal to one quarter of the wavelength of the highest frequency of interest. Another simple mesh method can be: (1) to give an initial element number that is reasonable and economic; and (2) to increase this number until converged results are obtained. The element numbers used in the calculations through this paper were determined by using this method.

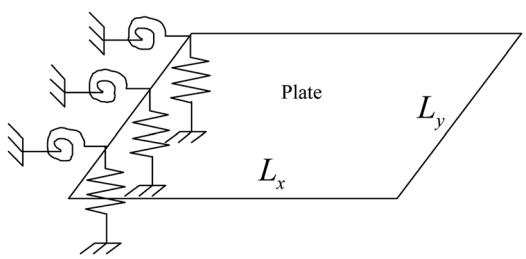

FIG. 1. A rectangular plate with elastic boundary supports along the edges (for simplicity and clarity, only the supports along the left edge are shown).

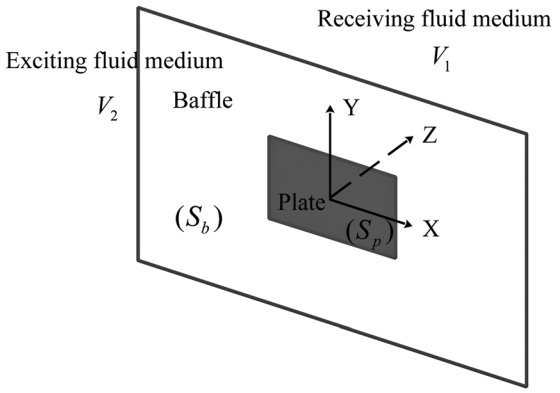

FIG. 2. A rectangular plate mounted on an infinite rigid baffle.

To integrate the finite element equation, Eq. (1), step-by-step in the time domain, the Newmark integration scheme[18] is used. The main assumptions of the Newmark method can be expressed as

$$\{\dot{u}(t+\Delta t)\} = \{\dot{u}(t)\} + [(1-\gamma)\{\ddot{u}(t)\} + \gamma\{\ddot{u}(t+\Delta t)\}]\Delta t, \tag{2}$$

$$\{u(t+\Delta t)\} = \{u(t)\} + \{\dot{u}(t)\}\Delta t + \left[\left(\frac{1}{2}-\alpha\right)\{\ddot{u}(t)\} + \alpha\{\ddot{u}(t+\Delta t)\}\right](\Delta t)^2, \tag{3}$$

where α and γ are Newmark parameters that can be determined in order to obtain integration accuracy and stability, and Δt is the time step. More details about this method and the choice of values of α and γ can be found in Ref. 18. Once the external load vector $\{F(t)\}$ is known, the vectors of the nodal displacement $\{u\}$, velocity $\{\dot{u}\}$, and acceleration $\{\ddot{u}\}$ can be solved using this method. Unless stated otherwise, $\alpha = 0.25$ and $\gamma = 0.5$ are used in the following numerical calculations.

2. Elastic boundary supports

The elastic boundary can be idealized by combining translational and rotational springs,[3,4,21,22] as shown in Fig. 1. The shear force Q and bending moment M_B produced by the springs of each edge can be written in terms of flexural displacement, translational stiffness S_t, and rotational stiffness S_r.[22] The stiffness matrices $\{K\}$ of the plate with elastic boundary supports in Eq. (1) is then given as

$$\{K\} = \{K_{\text{plate}}\} + \{K_{\text{edge}}\}, \tag{4}$$

where $\{K_{\text{plate}}\}$ is the plate's stiffness contribution to the stiffness matrix and $\{K_{\text{edge}}\}$ is the edge's stiffness contribution to the same matrix. Expressions for these matrices can be found in Ref. 3. In this study, translational stiffness S_t and rotational stiffness S_r have been nondimensionalized, as used in Refs. 3, 21, and 22.

The elastic parameters along the contour can be arbitrarily varied to reproduce simply supported ($S_t = \infty$ and $S_r = 0$), clamped ($S_t = \infty$ and $S_r = \infty$), free ($S_t = 0$ and $S_r = 0$), and guided ($S_t = 0$ and $S_r = \infty$) edges, or any intermediate situation (i.e., general elastic boundary conditions). Moreover, these parameters can vary spatially along each edge to represent arbitrary non-uniform elastic restraint. Unless stated otherwise, in the following numerical calculations the infinite large value is represented by a very large number, 1×10^{12}.

C. Sound radiation of the plate

The time-domain boundary integral equation used to describe the radiated sound field of the plate (Fig. 2) is given as[23]

$$C(\xi)p(\xi,t) = \int_S \int_0^t \sigma^*(x,t;\xi,\tau)p(x,\tau)d\tau dS - \int_S \int_0^t \sigma(x,t;\xi,\tau)\frac{\partial p(x,\tau)}{\partial n}d\tau dS, \quad (5)$$

where σ and σ^* are the fundamental pressure and fundamental flux, respectively, p is acoustic pressure, the coordinates x and ξ are the source and receiver points respectively, $C(\xi)$ is a constant[23] whose value depends on the location of the point ξ, t represents time, n is the unit normal direction on S, and S is the integration area, which includes both the baffle area S_b and the plate area S_p. The flux function $\partial p/\partial n$ can be expressed as $\partial p/\partial n = -\rho_0 \ddot{u}$, where ρ_0 is the fluid density, and $\ddot{u}$ is the normal acceleration of the plate.

In this paper, the plate is assumed to be flat and mounted on an infinite rigid baffle (see Fig. 2). Similar to the treatment in Ref. 24, the half-space fundamental pressure and flux solutions are adopted to avoid modeling of the infinite baffle. Equation (5) can then reduce to the well-known Rayleigh integral equation

$$p(\xi,t) = \int_{S_p} \int_0^t \rho_0 \sigma_H(x,t;\xi,\tau)\ddot{u}_n(x,\tau)d\tau dS_p, \quad (6)$$

where $\sigma_H = [1/(2\pi r)]\delta[t - (r/c) - \tau]$ is the half-space fundamental pressure solution in time domain. δ is the Dirac δ function, the distance function $r = |\xi - x|$, and c is the sound propagation speed. It is worth mentioning that Eq. (6) is valid for p either in the acoustic domain or on the surface S_p.

To solve Eq. (6), the plate surface S_p is discretized into a number of boundary elements. A time-marching scheme is then used to obtain the numerical solution for the unknown $p(\xi,t)$ at each discrete time step. A linear time interpolation function is employed in this scheme. More details about the numerical implementation procedure can be found in Ref. 23. Note that the singular integrals appear if the receiver point ξ exists on plate surface S_p. The methods to solve this singular integral can also be found in Ref. 23.

The discretization of the space and time variables are the same as those used in the TDFEM method, so that the radiated sound pressure can be solved by Eq. (6) when the vibration (acceleration) response is determined (by the TDFEM method).

III. MODEL VALIDATION

A. Validation of the prediction method against two existing measurements

We predicted the transient response of a single plate with different elastic boundary conditions and used two sets of existing experimental data with two different types of boundary conditions to validate the prediction method.

1. Measurement of NASA (Simply supported at all edges)

A simply supported glass window was used in the NASA sonic boom measurements in 2007.[14] The window had the dimension of 0.7 m × 1.2 m. The element numbers, time interval Δt, and damping ratio used in our numerical calculation were 6×10, 6.3 ms, and 0.08, respectively. Figure 3 shows the comparison between the predicted results and the experimental data provided by NASA. A good agreement can be seen in this figure. The receiving side in the model is assumed to be a sound-free field, which differs from the receiving side (a real bedroom) in NASA's experiment. The vibration (accelerometer) response data provided by NASA, however, could still be used to validate the model, since the reflected sound in the bedroom had little effect on the vibration motion of the window.

2. Measurement of Forsyth and Warburton (Clamped-free-free-free)

Forsyth and Warburton measured the transient displacement of a steel cantilever plate impacted by a small steel ball.[11] The plate was 16 inches long, 7.5 inches wide, and 0.282 inches thick, with one 7.5-inch edge clamped and the other edges free. The element numbers, time interval Δt, and damping ratio used in our numerical calculation were 32×16, 10 μs, and 9×10^{-5}, respectively. Figure 4 compares the predicted results and the experimental data and shows generally good agreement between them.

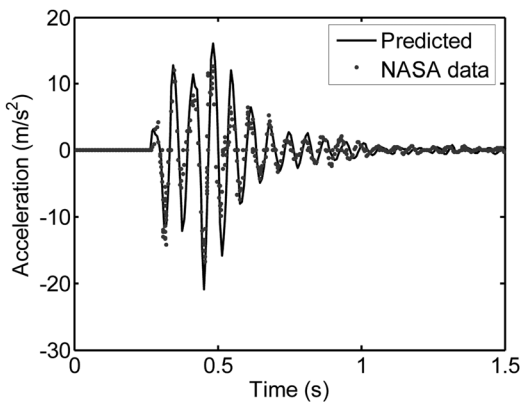

FIG. 3. Comparison of the predicted results (-) and experimental data of NASA (•) (Ref. 14).

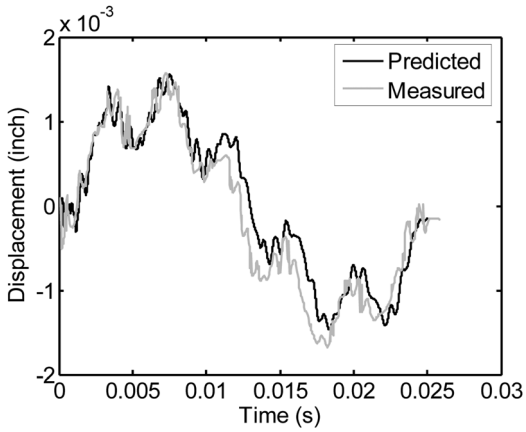

FIG. 4. Comparison of the predicted results (heavy color) and experimental data (light color) of Forsyth and Warburton (Ref. 11).

B. Validation of the prediction method against the authors' experimental measurement

The boundary conditions of the experiments shown in the previous subsection were both classical boundary conditions. To further validate the proposed model with more general boundary conditions, we measured the transient vibrations and sound radiations of a single plate with a non-classical boundary condition.

1. Experimental setup

Figure 5 schematically illustrates the experimental setup. We conducted measurements in two connected chambers at The Hong Kong Polytechnic University. The net volumes of these two chambers were 200 m^3 and 70 m^3, respectively. The larger chamber was used as the receiving room and the smaller chamber as the source room. The two chambers shared a common wall. This wall had a square port at its center sized 26 cm $\times$ 26 cm, which was designed to hold the tested panel. Acoustic absorptive materials were added to the surface of the walls of these two chambers except for the common wall. These absorptive materials were used to reduce as much as possible any reflected sound that may have acted on the tested panel in the source room. Absorptive materials were also used in the receiving room to ensure that the sound pressure measured in the receiving room would be completely radiated from the tested panel. A 1 mm thick aluminum (Al) panel was mounted in this port using two identical steel frames that screwed directly into the port. Each frame was 34 cm by 34 cm square and 3 mm thick, with a 24 cm by 24 cm square opening cut out of the middle. The Al panel was cut to 25.6 cm by 25.6 cm square to allow 8 mm of each edge to be clamped between these two steel frames. The wall and the steel frames were regarded as an infinite baffle.

A Kistler 9726A impact hammer was used to produce a transient impact force acting on the Al panel in the source room, while at the same time two B&K4935 microphones were put in the receiving room to measure the radiated sound, and a B&K 4394 accelerometer was attached to the Al panel to measure the acceleration. The two microphones, referred as "Mic 1" and "Mic 2," were located at the center line of the Al panel with 0.155 m and 1.112 m, respectively, away from the panel. A Cartesian coordinate system (X, Y, Z) was used in this paper, as shown in Fig. 5. The origin was set at the center of the Al panel. The locations (coordinates) of the impact point and the accelerometer were (−0.06, 0.06, 0) and (0, 0, 0) in unit meters, respectively, as shown in Fig. 5(b). All data were collected by PULSE (Type B&K 3160-B-042) at a sampling rate of about 8.2 kHz (0.12 ms) for a record length of 1 s.

2. Boundary condition and damping of the tested panel

The actual boundary condition and damping of the plate system used in this experiment need to be determined before the comparison between the predictions and experimental measurements can be performed. This plate system has been used in the authors' previous experimental work[25] that was a study on the frequency characteristics of sound transmission. The boundary parameters S_t and S_r and the damping ratio η were identified by the results from the modal testing, which are 3201, 13.28, and 0.0115, respectively. Details about their identification procedure can be found in Ref. 25.

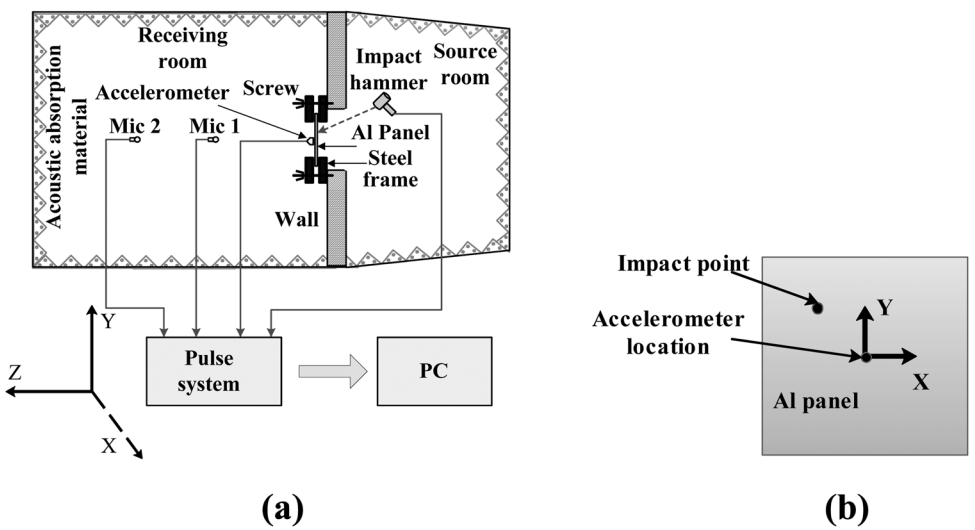

FIG. 5. Schematic diagram of the experimental setup. (a) Experimental setup (the plate system is enlarged in this figure for illustration). (b) Locations of the impact force and the accelerometer.

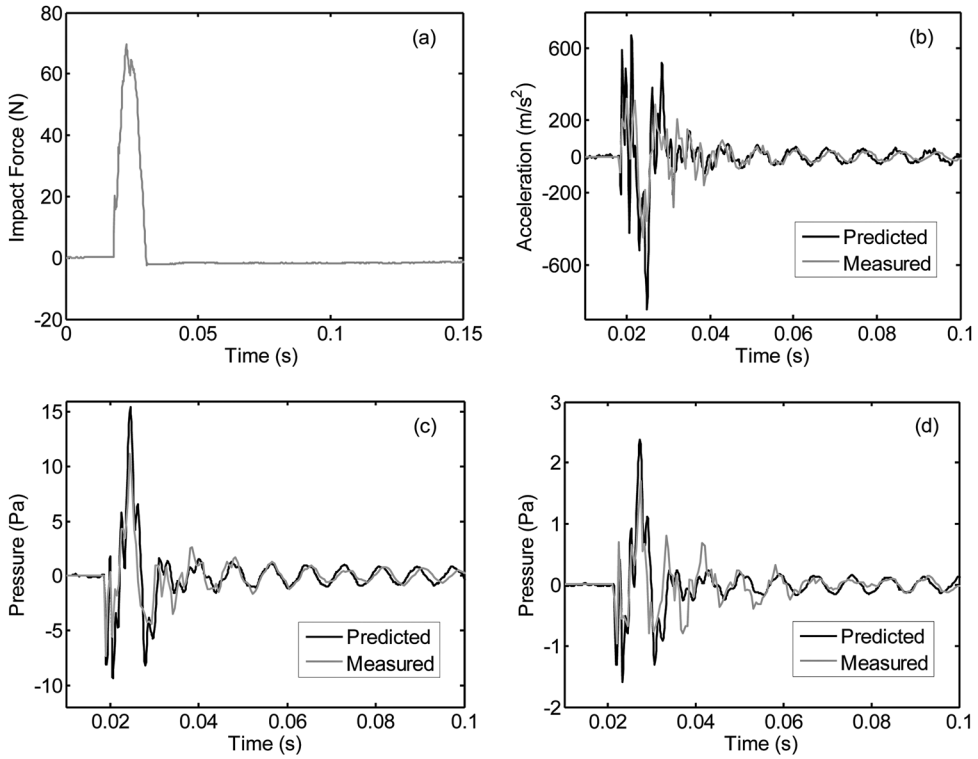

FIG. 6. Comparison of the predicted results (heavy color) and experimental data (light color). (a) Impact force time history. (b) Acceleration time history. (c) Pressure time history of "Mic 1." (d) Pressure time history of "Mic 2."

3. Experimental results and discussion

The time histories of the three measured parameters were the impact force, the acceleration of the panel, and the sound pressure in the receiving room. Figure 6 shows the measured results, denoted as [Fig. 6(a)] impact force, [Fig. 6(b)] acceleration, [Fig. 6(c)] sound pressure of "Mic 1," and [Fig. 6(d)] sound pressure of "Mic 2." We used the impact force shown in Fig. 6(a) as the input to the numerical model. For comparison, we also include the predicted results in Fig. 6(b)–6(d). The element numbers used in the numerical calculation were 8×8.

As Fig. 6 shows, the predicted vibration (acceleration) and sound radiation (sound pressure) results are in good agreement with the experimental data. The discernible discrepancies can be attributed to a number of factors, such as the uneven panel thickness, the non-uniform boundary conditions along the four edges, approximate damping, and the added mass caused by the accelerometer. In addition, only a rough location of the impact point was available when striking a hammer by hand. Also, the predicted sound pressure of "Mic 1" agrees better with the experimental data than the predicted results of "Mic 2"; this is because of the imperfect sound absorption at the boundaries of the receiving room, since the location of "Mic 2" was much further from the tested panel and nearer to other walls of the room.

IV. APPLICATIONS TO SONIC BOOM

Another objective of this work was to examine the effects of different boundary conditions on the transient vibration and sound radiation (TVSR) of a single-pane window caused by sonic booms. Using the proposed model, we carried out parametric studies on a single-pane glass window. The window was 1.3 m long, 0.9 m wide, and 1.5 mm thick. Young's modulus, density, Poisson's ratio, and damping factor were 65 GPa, 2500 kg/m^3, 0.25, and 0.04, respectively. The window was assumed to be with uniform boundary supports along the four edges and impacted by a 2 psf (95.6 pa), 150 ms N-wave, as shown in Fig. 7. The element numbers and time interval Δt used in the numerical calculation were 8×6 and 0.4 ms, respectively. Since the key concern in this study is the effect of the boundary supports rather than that of the wave incidence angle, in the following simulations the N-wave was assumed to be at normal incidence for simplify. However, it should be noted that for a realistic sonic boom any incidence angle is possible, and the actual incidence angle needs to be well estimated (or measured) since it can influence the final response.[17]

Figure 8 compares the responses of the window with all edges simply supported and with all edges clamped. To

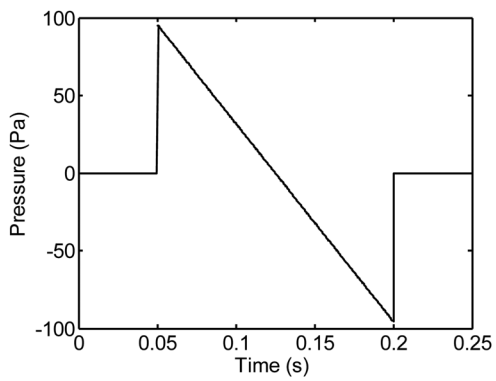

FIG. 7. Pressure time history of an N-wave.

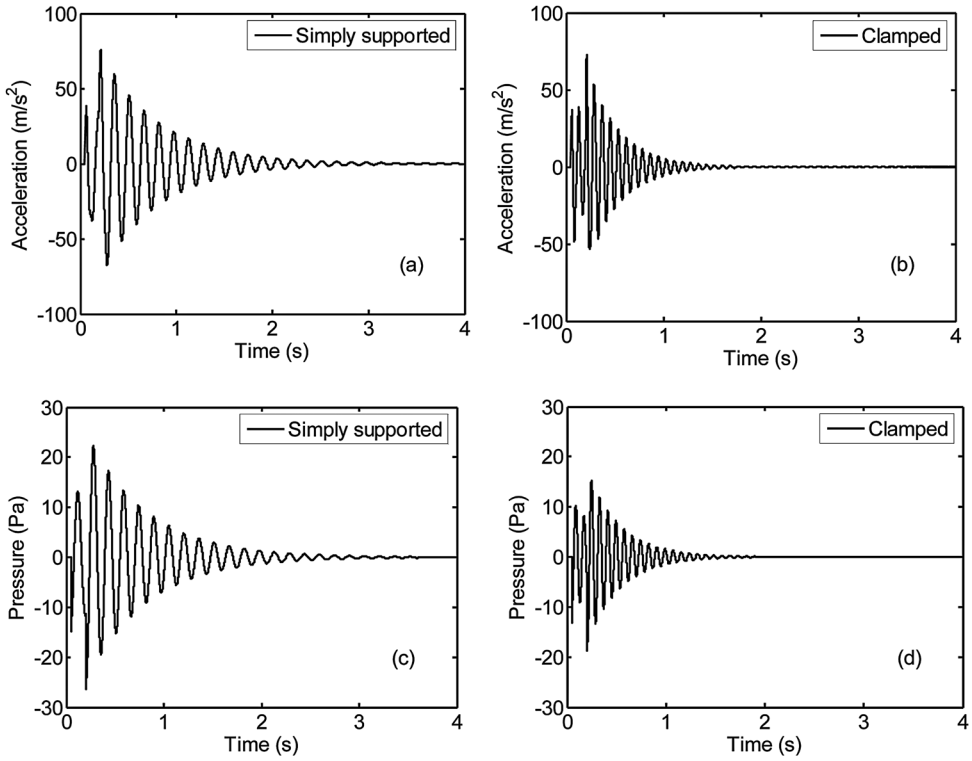

FIG. 8. Time-domain response of simply supported and clamped windows to the N-wave in Fig. 7. (a) Acceleration time history at point A on the simply supported window. (b) Acceleration time history at point A on the clamped window. (c) Pressure time history at point B radiated by the simply supported window. (d) Pressure time history at point B radiated by the clamped window. The coordinates of points A and B are (0, 0, 0) and (0, 0, 0.1) in unit meters, respectively. The coordinate system used here is the same as in Fig. 5.

make more comprehensive comparisons between these responses, we used a fast Fourier transform (FFT) to convert the responses into frequency spectrum data. Figure 9 shows the resulting one-third octave spectra, and as a benchmark, the criteria (thresholds) of tactile vibration[26] and non-audible acoustic perception.[27]

It can be seen in Fig. 8 that the time histories of TVSR of the clamped window changed more quickly and decayed more quickly than those of the simply supported window. This is because the TVSR responses of the clamped window contained more high-frequency components and fewer low-frequency components compared with those of the simply supported window, as shown in Fig. 9.

We also calculated more general boundary conditions such as the ones varying between simply supported and clamped edges. As noted by the authors in Refs. 28 and 29, these types of boundary conditions are common for practical windows in buildings. Since it is not clear which boundary

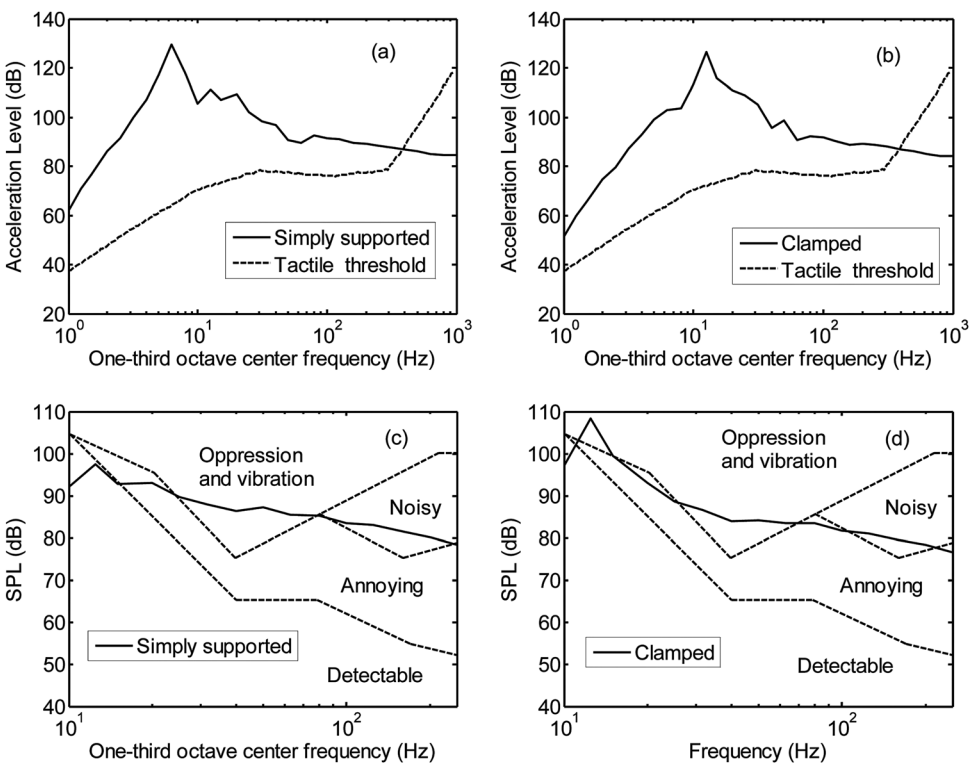

FIG. 9. Frequency-domain response of simply supported and clamped windows to an N-wave (solid line) and the corresponding evaluation criteria (dashed line). (a) Spectra of acceleration at point A on the simply supported window. (b) Spectra of acceleration at point A on the clamped window. (c) Spectra of pressure at point B radiated by the simply supported window. (d) Spectra of pressure at point B radiated by the clamped window. Points A and B are the same as those used in Fig. 8.

condition performs better (less vibration and noise) directly from the frequency spectrum figures such as Fig. 9, we applied some important criteria (thresholds) to evaluate the window's performance with different boundary conditions. These thresholds included the Hubbard tactile threshold[26] and the "oppressive and vibration" threshold.[27] We defined a variable EX related to the excess of the corresponding threshold, which can be expressed as follows:

$$EX(S_t, S_r) = \sum_f \{[R(S_t, S_r, f) - T(f)] \times y\}, \tag{7}$$

where

$$y = \begin{cases} 1, & \text{when } R(S_t, S_r, f) - T(f) > 0 \\ 0, & \text{else,} \end{cases}$$

f represents the center frequencies of the one-third octave bands, R is the spectrum of the acceleration (or sound radiation) in the one-third octave bands, and T is the Hubbard tactile threshold (or "oppressive and vibration" threshold). Responses that are peculiar to low frequency stimuli are feelings of oppression and vibration.[27] This is why we selected the "oppressive and vibration" threshold instead of other thresholds related to non-audible perception. Figure 10 shows the calculation results; we calculated parameters including maximum acceleration $A_{\max}$, maximum sound pressure $SPL_{\max}$, loudness (PLdB), EX_t, and EX_{op}. We calculated loudness (PLdB) using the method of Ref. 30, and EX_t, and EX_{op} according to Eq. (7), which represent the excesses of the Hubbard tactile threshold and the "oppressive and vibration" threshold, respectively. For better comparison, we normalized maximum acceleration $A_{\max}$, maximum sound pressure $SPL_{\max}$, EX_{op}, and EX_t in Fig. 10 by their maximum value and converted the corresponding results Q into decibels using the general definition $Q(\text{in dB}) = 20\log_{10}(Q)$.

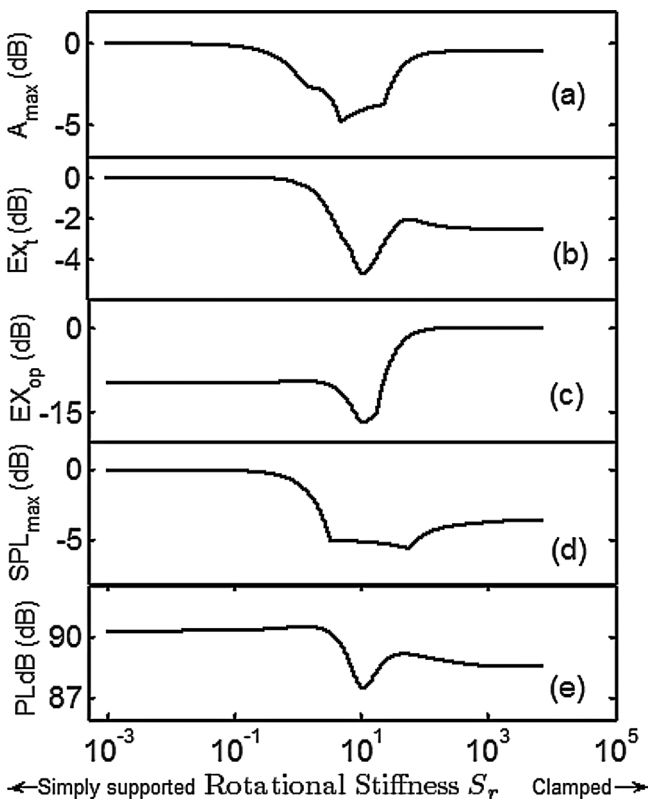

FIG. 10. The effects of different boundary conditions on the vibration and sound radiation of a window caused by an N-wave. (a) Maximum acceleration level at point A. (b) Excess of tactile threshold at point A. (c) Maximum sound pressure level at point B. (d) Loudness (PLdB) of the radiated sound at point B. (d) Excess of "oppressive and vibration" threshold at point B. Points A and B are the same as those used in Fig. 8.

In Fig. 10, the elastic boundary supports have a notable effect on the vibration and sound radiation from a window caused by an N-wave. In this case, there exists an optimum rotational stiffness value (around $S_r = 10$) at which the maximum acceleration $A_{\max}$, EX_t, loudness, maximum sound pressure level $SPL_{\max}$, and EX_{op} are minimized. As a result of this optimum rotational restraint treatment, reductions of 4 dB in vibration ($A_{\max}$), 5 dB in EX_t, 5 dB in sound radiation ($SPL_{\max}$), 3 dB in loudness (PLdB) and 16 dB in EX_{op} could be obtained in comparison with their maximum possible values.

V. CONCLUSION

We have developed a time-domain prediction method to examine the transient vibration and sound radiation of a rectangular window with general elastic boundary conditions. The approach used was based on the time-domain FEM and time-domain BEM methods. The predicted results agreed well with the experimental results for different types of boundary conditions.

We applied this method to evaluate the effects of elastic boundary supports on the response of a window caused by a sonic boom. The results show a significant effect of the elastic boundary supports on the window's TVSR. This study thus shows that maximum acceleration, tactile vibration perception, maximum radiated sound pressure, and non-audible perception levels can be effectively reduced using appropriate boundary conditions. Although the numerical examples in this study focused on the general boundary conditions that vary between simply supported and clamped edges, the current method could be applied to solve the transient vibroacoustic problems of any arbitrary uniform or non-uniform elastic edge supports.

[1]A. W. Leissa, *Vibration of Plates* (Acoustical Society of America, New York, 1993), Chap. 4.
[2]K. H. Kang and K. J. Kim, "Modal properties of beams and plates on resilient supports with rotational and translational complex stiffness," J. Sound Vib. **190**, 207–220 (1996).
[3]O. Chiello, F. C. Sgard, and N. Atalla, "On the use of a component mode synthesis technique to investigate the effects of elastic boundary conditions on the transmission loss of baffled plates," Comput. Struct. **81**, 2645–2658 (2003).
[4]J. Park, L. Mongeau, and T. Siegmund, "Influence of support properties on the sound radiated from the vibrations of rectangular plates," J. Sound Vib. **264**, 775–794 (2003).
[5]S. S. Mackertich and S. I. Hayek, "Acoustic radiation from an impulsively excited elastic plate," J. Acoust. Soc. Am. **69**, 1021–1028 (1981).
[6]E. B. Magrab and W. T. Reader, "Farfield radiation from an infinite elastic plate excited by a transient point loading," J. Acoust. Soc. Am. **44**, 1623–1627 (1968).
[7]I. Nakayama and A. Nakamura, "Mechanism of transient sound radiation from a circular plate for impulsive sound wave," J. Acoust. Soc. Jpn. **2**, 151–159 (1981).

[8]A. Akay and M. Latcha, "Sound radiation from an impact-excited clamped circular plate in an infinite baffle," J. Acoust. Soc. Am. **74**, 640–648 (1983).
[9]T. Takahagi and M. Nakai, "The approximation of pressure waveforms of impact sound radiation from clamped circular plates of various thicknesses," J. Acoust. Soc. Am. **78**, 2049–2057 (1985).
[10]I. Nakayama, A. Nakamura, and R. Takeuchi, "Transient radiation field from an elastic circular plate excited by a sound pulse," Acustica. **46**, 276–282 (1980).
[11]E. M. Forsyth and G. B. Warburton, "Transient vibration of rectangular plates," J. Mech. Eng. Sci. **2**, 325–330 (1960).
[12]A. Craggs, "Transient vibration analysis of linear systems using transition matrices," NASA-CR-1237, 1–24 (1968).
[13]Z. J. Fan, "Transient vibration and sound radiation of a rectangular plate with viscoelastic boundary supports," Int. J. Numer. Meth. Engng. **51**, 619–630 (2001).
[14]N. V. Sizov, K. J. Plotkin, and C. M. Hobbs, "Predicting transmission of shaped sonic booms into a residential house structure," J. Acoust. Soc. Am. **127**, 3347–3355 (2010).
[15]J. Mazumdar and J. R. Coleby, "Simplified approach to the vibration analysis of elastic plates due to sonic boom," J. Sound Vib. **45**, 503–512 (1976).
[16]A. Craggs, "The response of a simply supported plate to transient forces Part I: The effect of N-waves at normal incidence," NASA Contract. Rep. **1175**, 1–32 (1968).
[17]A. Craggs, "The response of a simply supported plate to 'N' waves at oblique incidence," J. Sound Vib. **16**, 293–307 (1971).
[18]D. C. Robert, S. M. David, E. P. Michael, and J. W. Robert, *Concepts and Applications of Finite Element Analysis*, 4th ed. (Wiley, New York, 2002), pp. 407–420, 536–538.
[19]D. J. Ewins, *Modal Testing: Theory, Practice and Application*, 2nd ed. (Research Studies Press, Baldock, 2000), pp. 62–64, 303–309.
[20]W. M. Kim, J. T. Kim, and J. S. Kim, "Development of a criterion for efficient numerical calculation of structural vibration responses," KSME Int. J. **17**, 1148–1155 (2003).
[21]A. Berry, J. L. Guyader, and J. Nicolas, "A general formulation for the sound radiation from rectangular, baffled plates with arbitrary boundary conditions," J. Acoust. Soc. Am. **88**, 2792–2802 (1990).
[22]W. L. Li, "Vibration analysis of rectangular plates with general elastic boundary supports," J. Sound Vib. **273**, 619–635 (2004).
[23]T. W. Wu, *Boundary Element Acoustics: Fundamentals and Computer Codes* (WIT Press, Southampton, UK, 2000), pp. 177–192.
[24]D. W. Herrin, F. Martinus, T. W. Wu, and A. F. Seybert, "An assessment of the high frequency boundary element and Rayleigh integral approximations," Appl. Acoust. **67**, 819–833 (2006).
[25]D. Y. Ou and C. M. Mak, "Experimental validation of the sound transmission of rectangular baffled plates with general elastic boundary conditions," J. Acoust. Soc. Am. **129**(6), EL274–EL279 (2006).
[26]H. H. Hubbard, "Noise-induced house vibrations and human perception," Noise Control Eng. J. **19**, 49–55 (1982).
[27]K. K. Hodgdon, A. A. Atchley, and R. J. Bernhard, "Low frequency noise study," Report No. PARTNER-COE-2007-001 Partner low frequency study group, (2007), pp. 16–17.
[28]J. D. Quirt, "Sound transmission through windows. I. Single and double glazing," J. Acoust. Soc. Am. **72**, 834–844 (1982).
[29]W. A. Utley and B. L. Fletcher, "The effect of edge conditions on the sound insulation of double windows," J. Sound Vib. **26**, 63–72 (1973).
[30]K. P. Shepherd and B. M. Sullivan, "A loudness calculation procedure applied to shaped sonic booms," NASA TP-3134 (1991), pp. 1–10.